Journal of Applied Polymer Science

Study on the poly(3-hydroxybutyrate-*co*−4-hydroxybutyrate)-based composites toughened by synthesized polyester polyurethane elastomer

Tianxiang Su,[1] Rui Zhang,[1,2] Jianjian Wang,[1] Wei Shao,[1,2] Yuan Hu[3]

[1]College of Chemical Engineering, Nanjing Forestry University, Nanjing, Jiangsu 210037, People's Republic of China

[2]Jiangsu Key Lab of Biomass-based Green Fuels and Chemicals, Nanjing Forestry University, Nanjing, Jiangsu 210037, People's Republic of China

[3]Suzhou Key Laboratory of Urban Public Safety, Suzhou Institute of University of Science and Technology of China, Suzhou, Jiangsu 215123, People's Republic of China

Correspondence to: R. Zhang (E-mail: zhangrui@njfu.edu.cn)

ABSTRACT: In this study, polycaprolactone(PCL)-based polyurethane (PU) elastomer containing 45 wt % hard segment component was synthesized and characterized by fourier transform infrared spectroscopy, gel permeation chromatography, and X-ray diffraction. As a toughening agent, the as-synthesized PU was incorporated into biodegradable poly(3-hydroxybutyrate-*co*-4-hydroxybutyrate) [P(3,4)HB] by solution casting to prepare P(3,4)HB/PU composites. The microstructure and properties of P(3,4)HB/PU composites were investigated using transmission electron microscopy, X-ray diffraction, tensile testing, scanning electron microscopy, differential scanning calorimetry, thermogravimetric analysis, and activated sludge degradation testing. The results show that PU can disperse well in a P(3,4)HB matrix. The elongation at break of P(3,4)HB/PU composites is remarkably increased while the yield strength and elastic modulus are decreased with an increase in PU content. At the same time, it is found that the fracture characteristic of P(3,4)HB is obviously transformed from brittleness into ductility with a gradual increase in PU loading. Moreover, the thermal stability of P(3,4)HB/PU composites is significantly improved compared with that of pure P(3,4)HB. In addition, the biodegradation rate of P(3,4)HB/PU composites is evidently reduced with the increase of PU content in the activated sludge degradation testing. © 2015 Wiley Periodicals, Inc. J. Appl. Polym. Sci. **2015**, *132*, 42740.

KEYWORDS: biopolymers & renewable polymers; composites; mechanical properties; polyurethanes

Received 2 August 2014; accepted 17 July 2015

DOI: 10.1002/app.42740

INTRODUCTION

With the considerably improved environmental awareness of society and concerns about the depletion of petrochemical based plastics, biodegradable plastic materials derived from renewable resources have attracted a great deal of attention.[1,2] As a typical kind of bioplastics, polyhydroxyalkanoates (PHAs) are synthesized and accumulated as intracellular carbon and energy storage material by many bacteria.[3,4] Owing to the outstanding properties, such as biodegradability, biocompatibility, excellent mechanical performance comparable with traditional petroleum-based plastics like polypropylene/(PP) and polyethylene/(PE),[5] PHAs have wide application prospects in the industrial, medical and agricultural fields.[6,7] Poly(3-hydroxybutyrate) (PHB), as a representative of the most extensively known PHAs, is a homopolymer with highly stereoregular structure and high crystallinity. Though the high crystallinity of PHB is useful in some areas, it leads to a stiffness–toughness imbalance which limits its application in many commercial fields.[8] Also, from a processing point of view, PHB not only has a very narrow processing window, but also undergoes extensive thermal degradation above its melting temperature during extrusion or injection molding.[9] When adding the comonomer unit 4-hydroxybutyrate (4HB), poly(3-hydroxybutyrate-*co*-4-hydroxybutyrate) [P(3,4)HB] can be fabricated. P(3,4)HB has a lower melt temperature and degree of crystallinity compared with PHB and its mechanical properties can change from stiff to soft with an increase of 4HB content.[10] However, the production cost increases a lot due to introducing of 4HB, so only P(3,4)HB with low 4HB content can be widely used in industrial fields. And the other disadvantages of P(3,4)HB with low 4HB content, such as slow crystallization rate, brittleness and low thermal stability, still limit its further application in some particular areas. Related studies showed that some nanofillers such as graphene,[11] calcium carbonate[12] and organoclay[13] can be

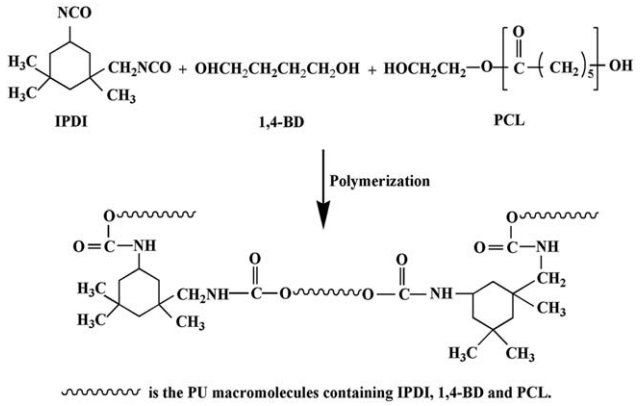

Figure 1. The reaction scheme for a single-step synthesis of PCL-based PU.

used to improve the mechanical and thermal properties of P(3,4)HB. In our previous study, cobalt–aluminum layered double hydroxide (LDH) and modified nanocrystalline cellulose (mNCC) were used as nanofillers to improve the properties of P(3,4)HB, including thermal stability and mechanical strength.[14,15] However, the inherent brittleness of P(3,4)HB with low content of 4HB is still a serious problem in these systems and there is little work reported on the toughening of P(3,4)HB so far. Therefore, it is necessary to develop an effective method to improve the toughness of P(3,4)HB.

Biodegradable polyurethane (PU) elastomer is an environmentally friendly material, which has been widely used as a toughening agent in polymer matrixes owing to its high elongation, moderate tensile strength, excellent abrasion and tear resistance.[16–18] The structure and properties of PU can be controlled comparatively easily by proper selection of polymer components, blend composition, and processing conditions.[19] As one of the synthesized polyester polyurethanes, polycaprolactone(PCL)-based polyurethane elastomers have excellent physical properties and biodegradability, which has attracted more and more attention.[20–23] However, to our knowledge, there is no information available in the literature about the use of synthesized PCL-based polyurethane elastomers as toughening agents in biodegradable polyesters including P(3,4)HB.

In this study, to obtain environmentally friendly P(3,4)HB based composites with good material performance, PCL-based PU elastomer was used as a toughening material to improve the mechanical properties of P(3,4)HB, especially ductility. Firstly, a linear polyester PU elastomer was synthesized by a moderate and effective method. Then, the as-synthesized PU was incorporated into P(3,4)HB matrix via solvent casting to prepare P(3,4)HB/PU composites. And, the microstructure and properties of P(3,4)HB/PU composites were further studied.

Table I. The Composition of P(3,4)HB/PU Composites

Designation	P(3,4)HB (wt %)	PU (wt %)
P(3,4)HB-0	100	0
P(3,4)HB-5	95	5
P(3,4)HB-10	90	10
P(3,4)HB-20	80	20
P(3,4)HB-30	70	30

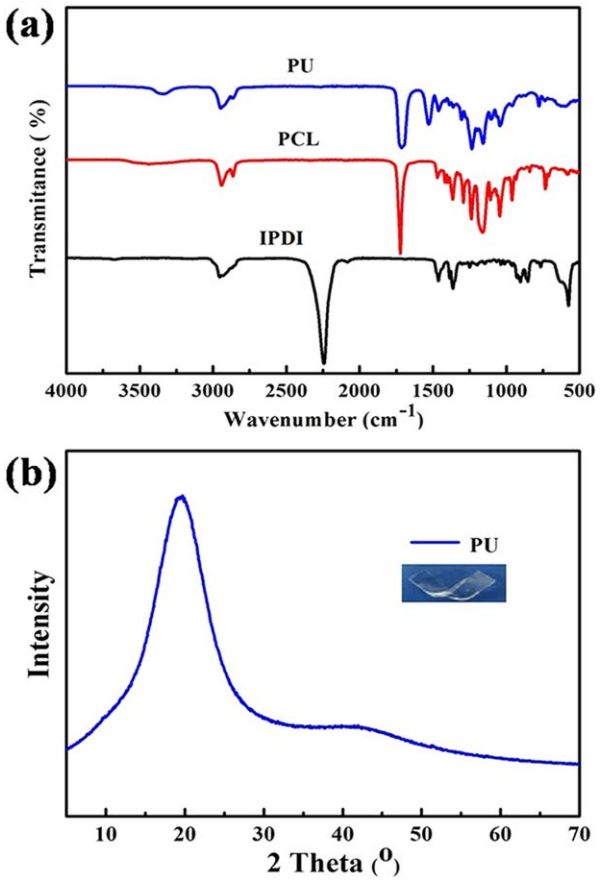

Figure 2. Characterization of the synthesized PU. (a) FT-IR spectra of PCL, IPDI and the synthesized PU; (b) X-ray diffraction pattern and actual photograph of the synthesized PU. [Color figure can be viewed in the online issue, which is available at wileyonlinelibrary.com.]

EXPERIMENTAL

Materials

The P(3,4)HB was purchased from Tianjin Green Bio-science (Tianjin, China). It exhibited a number average and weight average molecular weight of 1.33×10^5 g/mol and 2.63×10^5 g/mol, respectively, and the polydispersity was 1.97 (GPC analysis). The content of 4HB in the copolymer was 7.8 mol % as determined by ^{1}H-nuclear magnetic resonance (NMR) spectroscopy.

Isophorone diisocyanate (IPDI) was purchased from 9 Ding Chemistry (Shanghai, China) and poly(ε-caprolactone) diol (PLACCEL-210N, PCL) was obtained from Daicel Chemical Industries (Tokyo, Japan). 1,4-Butanediol (1,4-BD, analytical purity) was purchased from Shanghai Lingfeng Chemical Reagent (Shanghai, China). IPDI, 1, 4-BD and PCL were distilled under vacuum over 4Å zeolite. Other reagents were used without further purification.

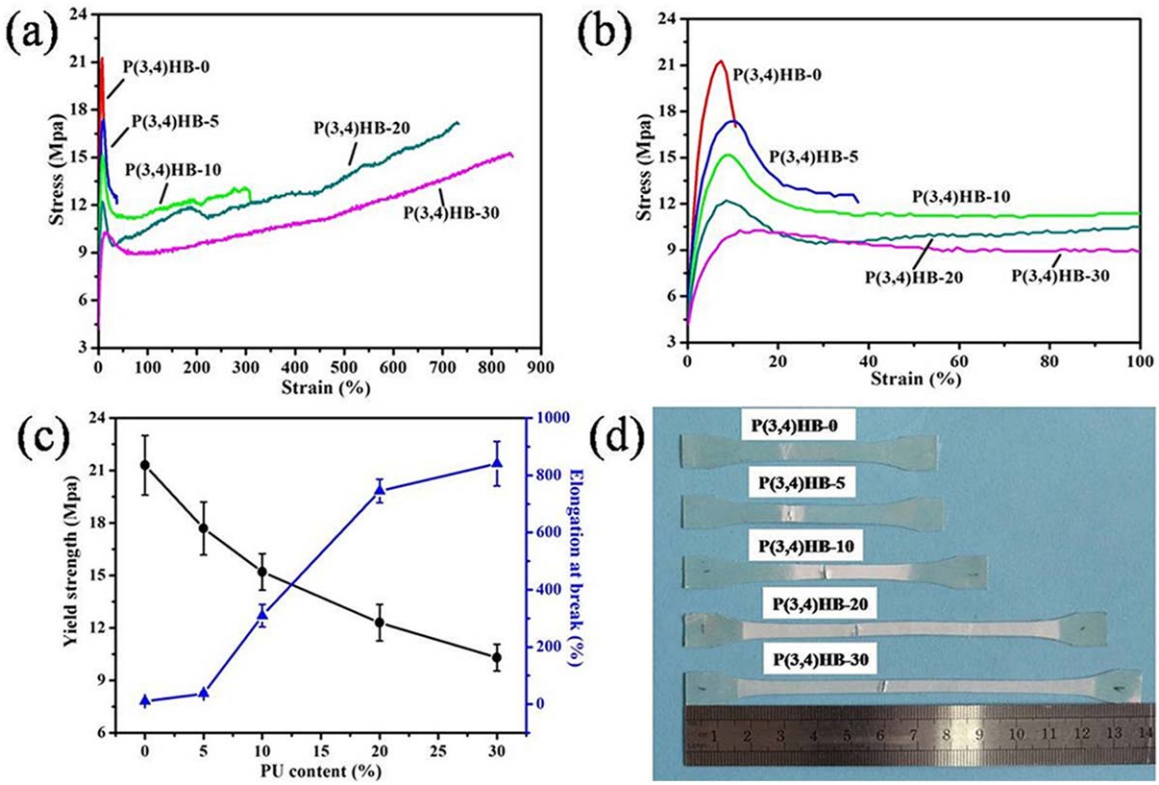

Figure 3. Tensile testing results for the P(3,4)HB/PU composites. (a) Stress–strain curves of P(3,4)HB/PU composites with different PU contents, and (b) enlarged part of the curves in image (a) near the yielding region; (c) yield strength and the elongation at break with different PU content; (d) photographs of P(3,4)HB/PU composites after tensile testing. [Color figure can be viewed in the online issue, which is available at wileyonlinelibrary.com.]

Synthesis of PU Elastomer

In order to obtain environmentally friendly P(3,4)HB based composites with good material performance, PCL-based PU elastomer was used as a toughening material to improve the mechanical properties of P(3,4)HB, especially ductility. Firstly, a linear polyester PU elastomer was synthesized by a moderate and effective method. Then, the as-synthesized PU was incorporated into P(3,4)HB matrix via solvent casting to prepare P(3,4)HB/PU composites. And, the microstructure and properties of P(3,4)HB/PU composites were further studied.

The formula and symbols for the synthesized PU with 45 wt % hard segment component are shown in Figure 1. In this synthesis reaction, poly(ε-caprolactone) diol (PCL) was used as soft segment, isophorone diisocyanate (IPDI) and 1, 4-butanediol (1, 4-BD) were used as hard segment, with 1, 4-butanediol (1, 4-BD) being a chain extender in this reaction. The total molar ratio of isocyanate ester groups (N=C=O) of IPDI and hydroxyl groups (-OH) of PCL and 1, 4-BD was 1 : 1, and the content of hard component (45 wt %) can be calculated according to the weight of hard segment divided by the total mass.

The experiment is as follows: PCL (0.01 mol), 1, 4-BD (0.019 mol) and IPDI (0.029 mol) were added to a 100 mL round-bottom flask. The reaction mixture was heated at 80oC under nitrogen atmosphere with continuous magnetic stirring for 3 h. Then the reaction liquid was transferred quickly into a polypropylene mold, and the product was placed in vacuum oven at 125oC for 24 h to complete the chain extension giving a polyester PU containing 45 wt % hard segment.

Preparation of P(3,4)HB/PU Composites

A certain amount of dried P(3,4)HB powder and the PU were added to 50 mL chloroform. The proportions of P(3,4)HB and

Table II. The Results of Tensile Testing for Neat P(3,4)HB and Its Composites

Designation	Yield strength (MPa)	Fracture strength (MPa)	Elogation at break (%)	Elastic modulus (MPa)
P(3,4)HB-0	21.3 ± 1.7	16.7 ± 0.7	10.4 ± 0.6	601.9 ± 45.6
P(3,4)HB-5	17.7 ± 1.5	12.5 ± 0.9	36.9 ± 5.9	471.5 ± 23.9
P(3,4)HB-10	15.2 ± 1.0	13.2 ± 1.1	309.2 ± 38.9	417.7 ± 24.1
P(3,4)HB-20	12.3 ± 1.0	16.8 ± 1.7	745.3 ± 41.1	239.4 ± 37.4
P(3,4)HB-30	10.3 ± 0.8	15.1 ± 0.9	840. 8 ± 77.6	129.5 ± 10.9

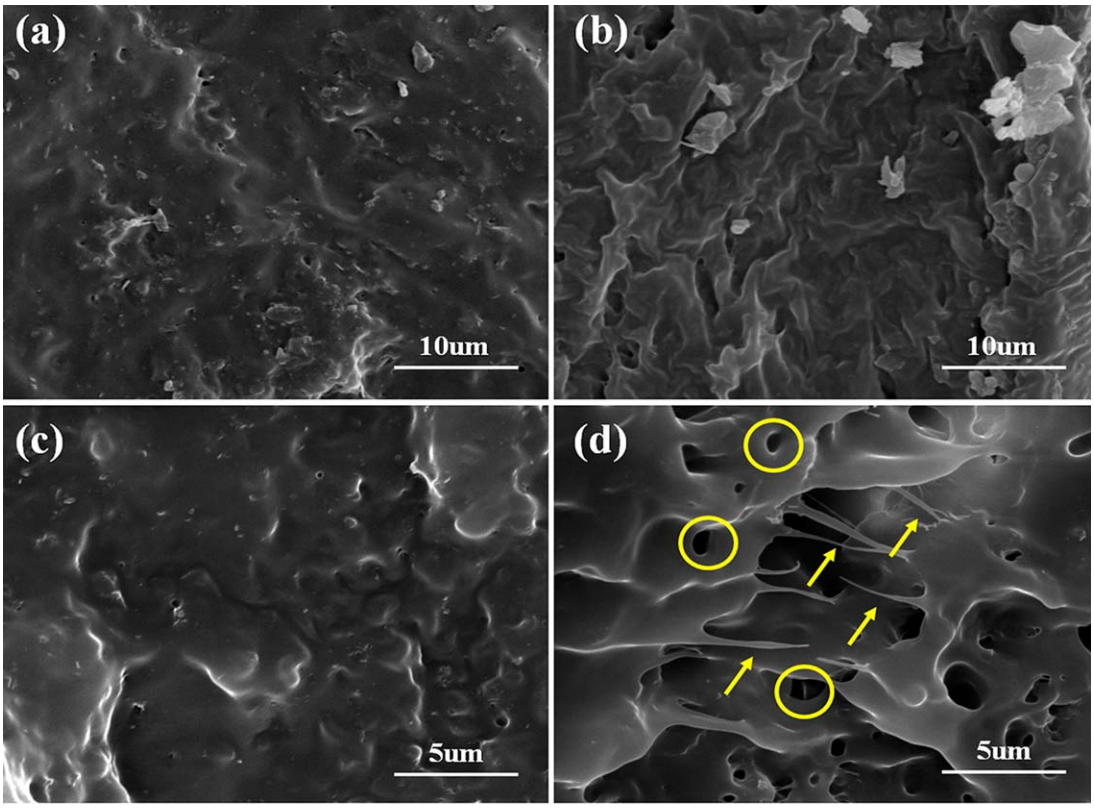

Figure 4. SEM images of the fracture surfaces of the P(3,4)HB/PU composites. (a) P(3,4)HB-0 and (b) P(3,4)HB-30 fractured in liquid nitrogen; (c) P(3,4)HB-0 and (d) P(3,4)HB-30 fractured in tensile tests. [Color figure can be viewed in the online issue, which is available at wileyonlinelibrary.com.]

PU are shown in Table I. The mixture was treated with continuous stirring at 25°C for 24 h to dissolve it completely. Then the solution was cast into a Teflon mold and evaporated overnight at ambient temperature to obtain P(3,4)HB/PU composite films. The resulting films were further dried in vacuum at 40°C for one week to entirely remove the residual solvent. The resulting films, with a thickness of about 0.1 mm, were stored at ambient temperature for two weeks to obtain stable properties before conducting further tests.

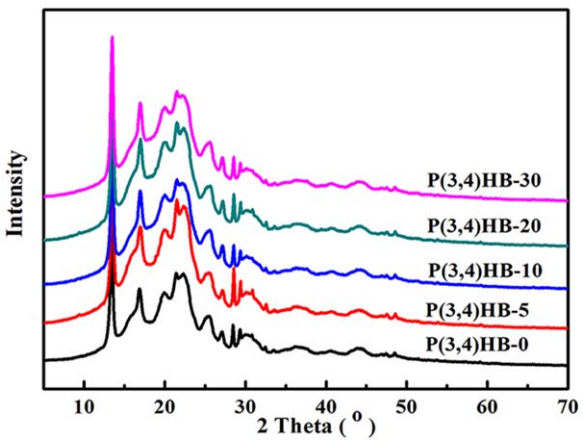

Figure 5. X-ray diffraction patterns of neat P(3,4)HB and P(3,4)HB/PU composites. [Color figure can be viewed in the online issue, which is available at wileyonlinelibrary.com.]

Characterization and Measurements

Fourier transform infrared spectroscopy (FT-IR) measurements were performed using a Perkin Elmer spectrometer model Spectrum Two (Perkin Elmer Instruments, USA). Spectra of the samples were obtained by averaging 15 scans with a wavenumber range of 4000 to 500 cm^{-1} and a resolution of 2 cm^{-1}.

Gel Permeation Chromatography (using an Agilent Technologies 1260 Infinity chromatograph, United States) was used to determine the relative molecular weight and polydispersity of the polymers. Weight average molecular weight (M_w), number average molecular weight (M_n) and polydispersity (M_w/M_n) were obtained based on polystyrene standards. All the tests were performed at 25°C and chromatographic grade tetrahydrofuran was used as organic solvent.

X-ray diffraction (XRD) was employed on a Japan Ultima IV X-ray diffractometer with Cu K_α radiation ($\lambda = 0.154178$ nm) in the range of 5°∼ 70°.

TEM was carried out using a JEOL (Tokyo, Japan) JEM-100SX TEM with an acceleration voltage of 100 kV. The specimens were cut into ultrathin slices at room temperature with an ultramicrotome (Ultracut-1, UK) equipped with a diamond knife.

Mechanical property testing was performed at 25°C with a crosshead speed of 50 mm/min based on GB/T 1040.3–2006 standard using a SANS testing machine (Shenzhen SANS Mechanical Company, China). All the specimens were manufactured using a

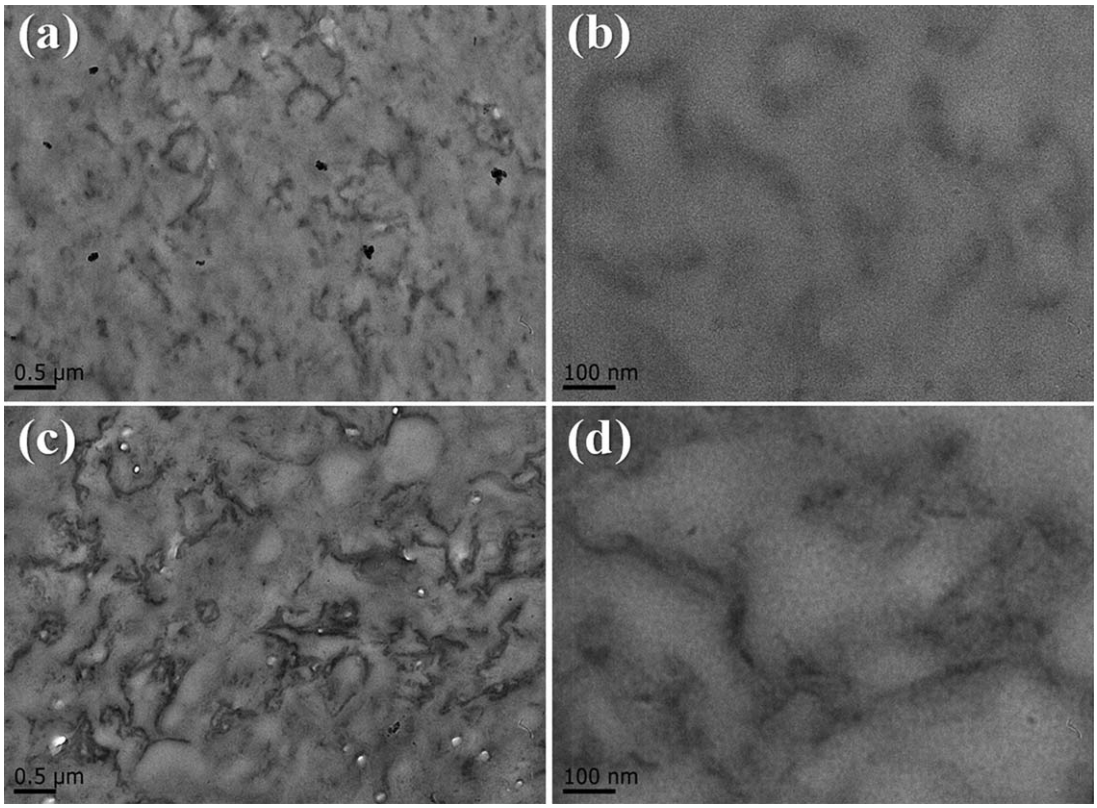

Figure 6. TEM image of P(3,4)HB/PU composites: low magnification (left) and higher magnification (right): (a) and (b) P(3,4)HB-5; (c) and (d) P(3,4)HB-20.

dumbbell-shaped mould with a dimension of 75 × 5 × 0.1 mm^3. At least five specimens were tested for each sample to obtain an average value.

DSC analysis was employed to examine the thermal transitions of the composites on a DSC instrument (Netzsch 200 F3) under nitrogen atmosphere. Samples of about 8 mg were placed in sealed aluminum crucibles. P(3,4)HB/PU composites were scanned over a range of −50°C to 200°C (10°C/min for heating and 20°C/min for cooling) after a pretreatment of heating to 200°C and equilibration at 200°C for 2 min to eliminate thermal and stress histories. Different heating rates (5, 10, 15, and 20°C/min) was used to demonstrat the melt recrystallisation process of P(3,4)HB.

To better understand the crystallization behavior, P(3,4)HB and P(3,4)HB/PU composites were studied using a polarized optical microscope (POM) equipped with a hot stage and a digital camera (Nikon model eclipse E400 pol). The samples were heated from room temperature to 200°C between two glass slides and equilibrated at this temperature for 2 min, then cooled to 50°C to crystallize isothermally.

Thermogravimetric analysis (TGA) was performed on a Q5000IR thermogravimetric analyzer instrument (TA Instruments) to determine the thermal stability of the composites. About 5 mg of samples were placed in a Pt pan and heated at temperature ranging from 30°C to 600°C with a heating rate of 10°C/min under flowing nitrogen (60 mL/min). The reproducibilities of the mass loss and temperature data were ±0.2% and ±1°C, respectively.

Scanning electron microscopy (SEM) was carried out on an FEI Quanta-200 at an accelerating voltage of 20 kV to study the morphological features of the composites. The samples fractured in liquid nitrogen and fractured after tensile testing were first gold-plated before measurement.

The activated sludge degradation test of neat P(3,4)HB, PU and the composites were carried out in a basal medium. The activated sludge was obtained from a textile wastewater treatment plant and the basal medium used in all experiments was as described and supplied by Yu.[24] The initial sludge concentration was 2.1 g MLSS (mixed liquor suspended solids) per liter. The basal medium used in all experiments (unless indicated otherwise) contained the following (unit in milligrams per liter): K_2HPO_4 (1,112), KH_2PO_4 (2,088), glucose (940), $NaHCO_3$ (5,000), NH_4Cl (280), $MgSO_4{\cdot}7H_2O$ (100), yeast extract (100), and 1 ml of a trace element solution containing (milligrams per liter): $CaCl_2{\cdot}2H_2O$ (10), H_3BO_3 (0.05), $FeCl_2{\cdot}4H_2O$ (2), $ZnCl_2$ (0.05), $MnCl_2{\cdot}4H_2O$ (0.05), $CuCl_2{\cdot}2H_2O$(0.03), $(NH_4)_2SeO_3{\cdot}5H_2O$ (0.05), $AlCl_3{\cdot}6H_2O$ (2), $NiCl_2{\cdot}6H_2O$ (0.05), EDTA (1), and resazurin (0.2). 5 mL initial sludge was added to 100 mL basal medium in erlenmeyer flask with a stropper and the degradation process was implemented in a shaking bath and the temperature was 30°C. The specimens (10 × 10 × 0.1 mm^3) were placed in erlenmeyer flask containing activated sludge suspension. The degradation of the samples was initiated by the addition of basal medium. The degraded films were washed with distilled water every 2 days for t days. Then the films were dried completely and weighed. The surface morphology of the films was observed by optical

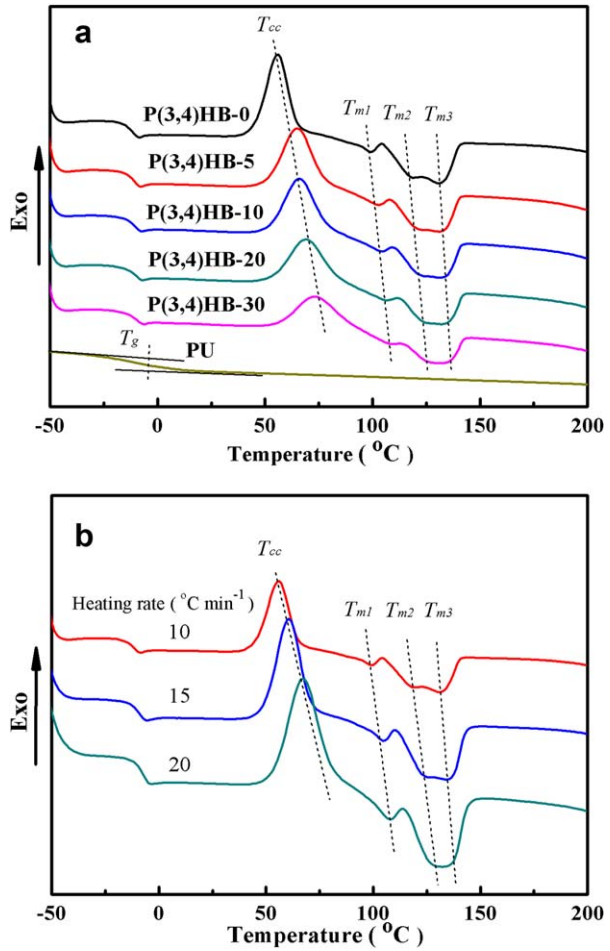

Figure 7. (a) Second heating traces in DSC of neat P(3,4)HB, PU and P(3,4)HB/PU composites. (b). Second heating traces in DSC of neat P(3,4)HB at different heating rates. [Color figure can be viewed in the online issue, which is available at wileyonlinelibrary.com.]

microscope. The degree of degradation was obtained from the weight loss in equation (1):

$$\text{Weight loss} = \frac{W_0 - W_t}{W_0} \times 100\% \quad (1)$$

Here W_0 is the dry weight before degradation and W_t is the dry weight after t days.

RESULTS AND DISCUSSION

Characterization of the Synthesized PU Elastomer

The FT-IR spectra of PCL, IPDI and the synthesized PU are given in Figure 2(a). Compared to PCL, the spectrum of PU has two extra peaks at around 1528 cm^{-1} and 3400 cm^{-1}, which is attributed to the C−N−H vibration and N−H stretching absorption of the urethane group. Furthermore, compared to IPDI, the stretching vibration peak of the N=C=O groups corresponding to the unreacted urethanes at 2240 cm^{-1} disappeared in the curve of PU, which indicates that the N=C=O groups have reacted with −OH of PCL and 1,4-BD completely. All the changes confirm that the polyester PU was successfully synthesized.

Gel permeation chromatography (GPC) was used to determine the relative molecular weight and polydispersity of the synthesized PU. The result shows that the number average molecular weight (M_n) of PU is 2.67 × 10^4 g/mol, the weight average molecular weight (M_w) of PU is 5.53 × 10^4 g/mol and the polydispersity index is 2.07.

X-ray diffraction analysis (XRD) is an effective method to study the microstructure of polymer materials. The XRD pattern of the synthesized PU containing 45 wt % hard segment component is shown in Figure 2(b). It can be seen that there are both large and small broad crystal diffraction peaks corresponding to 2θ=18° and 42°, which are associated with the amorphous phase of PU. One reason is that, as the soft segment of the PU, the molecular weight of PCL is only 1000 g/mol, which is not high enough to allow PU to form a crystalline morphology. The other is that, as a hard segment, IPDI is also difficult to crystallize due to the existence of isomers and its highly asymmetric molecular structure. As a result, the synthesized PU sample is transparent and flexible, as shown in the inset picture in Figure 2(b), in accordance with its amorphous structure.

Mechanical Properties of P(3,4)HB/PU Composites

As is well known, the inherent brittleness of P(3,4)HB with a low content of 4HB is a serious problem in application. So, the key to effective modification of P(3,4)HB for practical use is to improve its mechanical properties, especially ductility. Figure 3 gives the stress-strain curves of P(3,4)HB/PU composites and the data obtained are listed in Table II, which show that neat P(3,4)HB is brittle, with a yield strength of 21.3 MPa and elongation at break of only about 10.4%. It can be clearly seen that the elongation at break of P(3,4)HB/PU composites is markedly increased, while the yield strength and elastic modulus are decreased, with an increase in PU content. It can also be found that the fracture characteristic of P(3,4)HB is obviously transformed from brittleness into ductility with the gradual increase of PU loading. Compared with the neat matrix, P(3,4)HB-30, with a PU loading of 30%, has a much higher elongation at break of 840.8% and its yield strength drops significantly to 10.3 MPa. During stretching, distinct stress whitening and necking phenomena are observed [Figure 3(d)], which is a characteristic of ductile fracture. In Figure 3(a) it is very interesting to find that, after yielding occurred, the strain developed continuously while the stress continued to rise until broken, which means P(3,4)HB/PU composites have excellent tear resistance. Compared with neat P(3,4)HB, the composites are finally broken at a higher elongation [Figure 3(c)], which means that the synthesized PU has distinct toughening effect. Moreover, the modulus of P(3,4)HB/PU composites are gradually decreased with the addition of PU due to the lower moduli of PU compared to that of P(3,4)HB. From the above results, it can be concluded that the addition of PU can significantly improve the mechanical properties of P(3,4)HB.

To better understand the toughening effect of PU on P(3,4)HB/PU composites, the morphology of broken regions of the tensile tested specimens and samples fractured in liquid nitrogen (neat

Table III. DSC Results for Neat P(3,4)HB and Its Composites

Sample	T_g (°C)	T_{cc} (°C)	ΔH_{cc} (J/g)	ΔT_{cc} (°C)	T_{m1} (°C)	T_{m2} (°C)	T_{m3} (°C)
P(3,4)HB-0	−12.5	55.9	39.8	12.1	99.5	117.7	132.6
P(3,4)HB-5	−12.4	64.9	28.3	15.3	102.7	119.2	133.9
P(3,4)HB-10	−12.1	67.9	23.6	16.5	105.0	121.0	135.2
P(3,4)HB-20	−11.8	69.1	17.5	25.9	106.2	122.7	136.0
P(3,4)HB-30	−11.5	72.9	19.4	22.5	107.7	124.5	136.6
PU	− 4.1	/	/	/	/	/	/

ΔT_{cc}: the width of the peak T_{cc}.

P(3,4)HB and P(3,4)HB-30) was observed by SEM. From the images shown in Figure 4(a,c), it can be seen that neat P(3,4)HB has a smooth fracture surface due to the lack of large scale plastic deformation, indicating a typical brittle fracture behavior. As for the images shown in Figure 4(b,d), the fracture surfaces of P(3,4)HB/PU composites become rough and rugged, which implies a ductile fracture behavior. Furthermore, compared with image (c), there are two major differences observed in image (d). One is that there are many cavitations formed during the tensile testing process as shown in image (d), which are derived from the distortion and enlargement of micropores remained when the solvent evaporated during the preparation process of polymer. The other is that the fibrillar structure emerges with obvious tearing cracks and pulling fibres as shown in image (d), which are caused by the orientation of PU macromolecular chains during the stretching process. The above results confirm that PU has had a dramatic toughening effect on the P(3,4)HB matrix.

Microstructure of P(3,4)HB/PU Composites

To further understand the mechanism of the toughening effect, the microstructure of P(3,4)HB/PU composites and the dispersity of PU within the P(3,4)HB matrix were investigated using XRD and TEM. Figure 5 shows the WAXS patterns of P(3,4)HB/PU composites. The neat P(3,4)HB presents multiple peaks, which are consistent with those of pure PHB, indicating that only the PHB crystal structure is present in P(3,4)HB.[25,26] The main characteristic diffraction peaks are at around 13.5, 17.0, 22.0, 25.6, and 27.0°, corresponding to the crystallographic planes of (020), (110), (111), (121), and (040), respectively. In the case of P(3,4)HB/PU composites, the diffraction peaks are almost the same as those of neat P(3,4)HB, regardless of PU content, which indicates that the crystal structure of P(3,4)HB does not change. These results show the PU has no evident effect on the crystal structure of P(3,4)HB in the composites. A similar phenomenon has been reported previous studies using PHBV.[27]

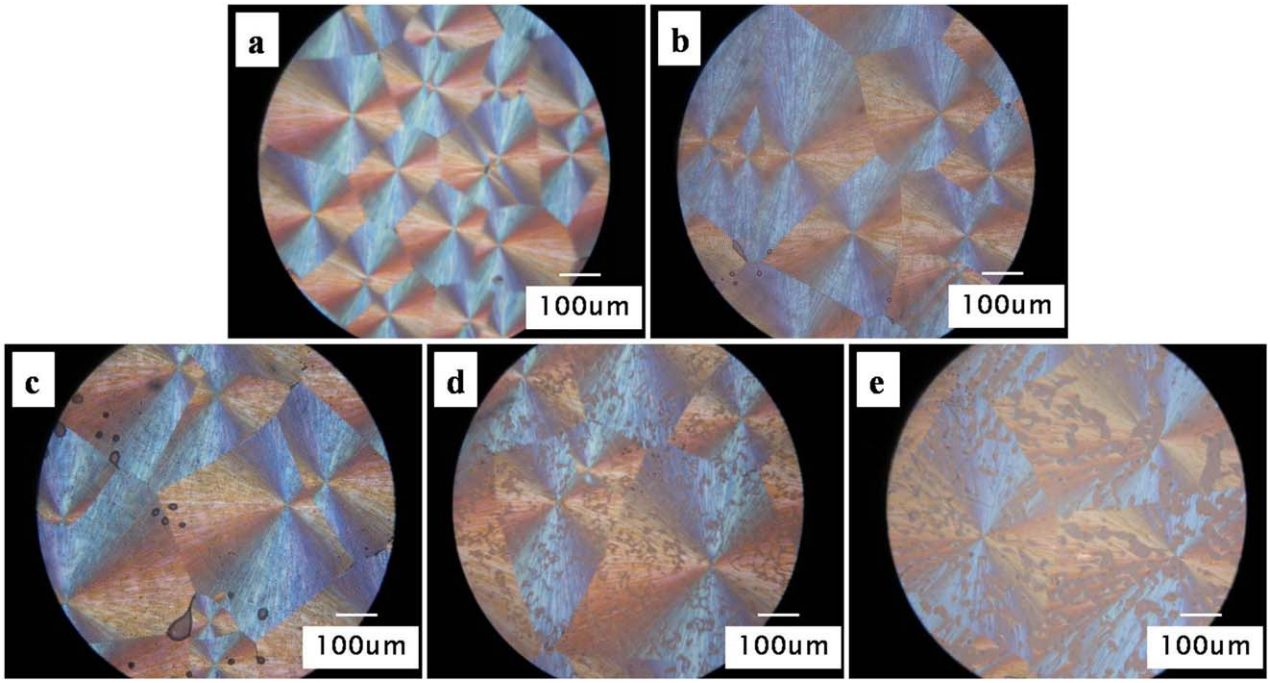

Figure 8. POM pictures of P(3,4)HB and P(3,4)HB/PU composites: (a) P(3,4)HB-0; (b) P(3,4)HB-5; (c) P(3,4)HB-10; (d) P(3,4)HB-20; (e) P(3,4)HB-30. [Color figure can be viewed in the online issue, which is available at wileyonlinelibrary.com.]

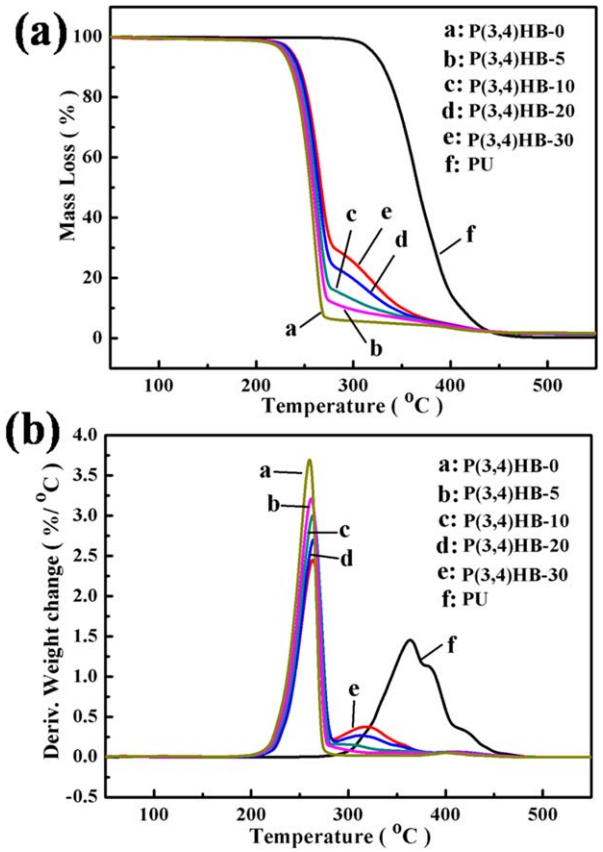

Figure 9. TG (a) and DTG (b) curves for PU and P(3,4)HB/PU composites. [Color figure can be viewed in the online issue, which is available at wileyonlinelibrary.com.]

The TEM images of P(3,4)HB/PU composites are shown in Figure 6. A two-phase morphology is found in all images, in which PU (black areas) is well dispersed on the nanometer scale in P(3,4)HB (white areas). Obviously, the continuous two-phase structure, namely "sea-sea" structure is formed, which is favorable for the delivery and dispersion of stress, and contributes to increasing the toughening effect of PU. Moreover, the physical interactions between the molecular chains of P(3,4)HB and PU, such as the hydrogen bonding between the C=O groups from P(3,4)HB and the N-H groups from PU, retard the agglomeration of the PU molecule, which may conduce it to disperse in the matrix. As a result, good dispersity and plastic deformation

Table IV. TG and DTG Data for Neat P(3,4)HB and Its Composites

Sample	Onset degradation temperature (T_{onset}/°C)	DTG Peak temperature (T_{max}/°C)
PU	320.2	363.8
P(3,4)HB-0	227.7	259.9
P(3,4)HB-5	230.0	261.5
P(3,4)HB-10	232.1	263.2
P(3,4)HB-20	235.4	264.8
P(3,4)HB-30	236.7	265.3

T_{onset}: the temperature at 5 wt % mass loss.

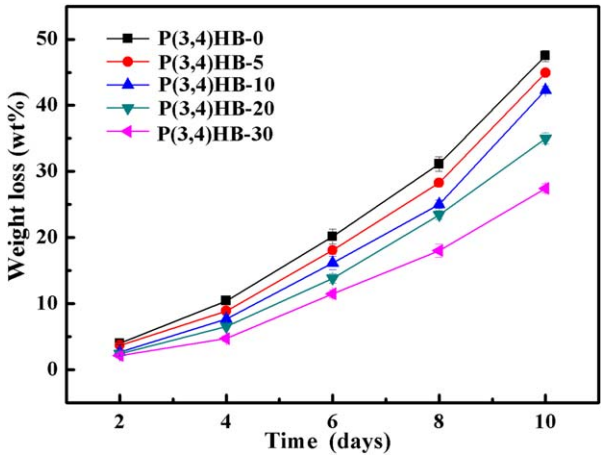

Figure 10. The weight loss curves of P(3,4)HB/PU composites after activated sludge degradation. [Color figure can be viewed in the online issue, which is available at wileyonlinelibrary.com.]

induced by energy dissipation are conducive to the improvement of toughness of P(3,4)HB/PU composites.

Crystallization Properties of P(3,4)HB/PU Composites

DSC measurement is used to determine the thermal transition and crystallization behavior of materials. As shown in Figure 7(a) and Table III, the glass transition, cold crystallization, and multiple melting of P(3,4)HB/PU composites can be clearly seen. Neat P(3,4)HB exhibits a glass transition temperature (T_g) at −12.5°C, an exothermic cold crystallization peak at 55.9°C and three endothermic melting peaks at 99.5, 117.7 and 132.6°C, respectively. The value of T_g of all P(3,4)HB/PU composites is between P(3,4)HB (T_g= −12.5°C) and PU (T_g= −4.1°C). Compared with neat matrix, there is a slight increase in glass transition temperature (T_g) of P(3,4)HB/PU composites with the addition of PU.

It can also be seen that the incorporation of PU remarkably increases the cold crystallization temperature (T_{cc}) and broadens the exothermic peak (ΔT_{cc}), indicating the crystallization ability of P(3,4)HB is decreased. Because of the interactions between the molecular chains of P(3,4)HB and PU, the energy barrier may be increased, which will reduce the mobility and reorganization of P(3,4)HB. At the same time, the area of crystallization peaks is reduced with the increasing content of PU, indicating that the crystallinity of composites is decreased with the adding of amorphous PU. The width of crystallization peaks is also increased with the addition of PU, showing that less perfect crystals are formed.

Multiple endothermic melting peaks are observed in all samples as shown in Figure 7(a), which demonstrates the melting-recrystallization-melting process.[28,29] And, from the DSC curves of neat P(3,4)HB at different heating rates as shown in Figure 7(b), the existence of multiple endothermic melting peaks can also be seen, which are responsible for the melting-recrystallization-melting process. The reason is that the crystallization of P(3,4)HB during melting process is incomplete and P(3,4)HB has lower homogeneous nucleation rate, resulting in domains that have different compositional distribution, with some being more enriched

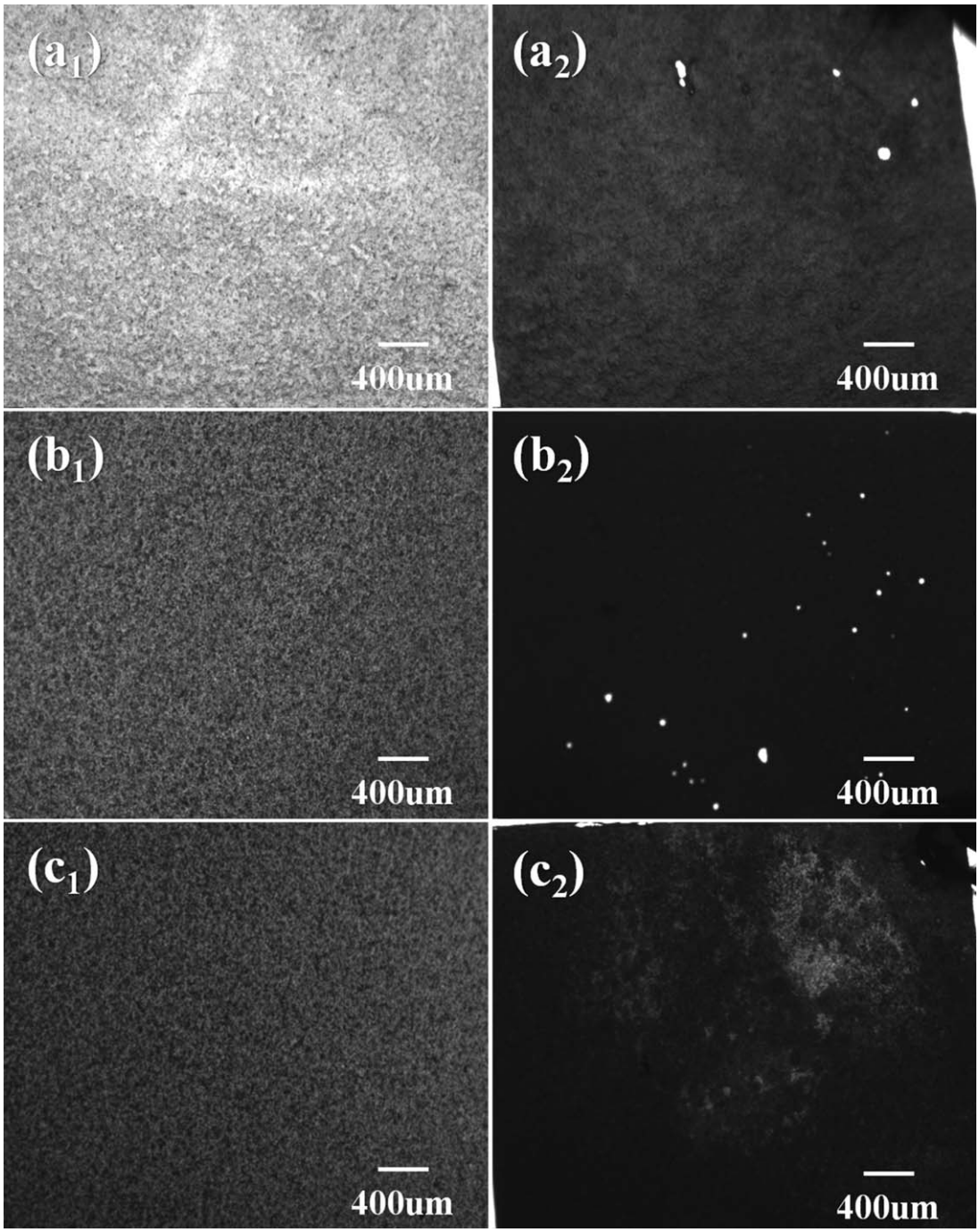

Figure 11. Optical microscope images of the surfaces of P(3,4)HB/PU composites before and after activated sludge degradation: (a_1) P(3,4)HB-0, (b_1) P(3,4)HB-5 and (c_1) P(3,4)HB-20 before degradation; (a_2) P(3,4)HB-0, (b_2) P(3,4)HB-5 and (c_2) P(3,4)HB-20 after degradation.

in the 4HB monomer unit and others being more enriched in the 3HB monomer unit. Thus, the less perfect crystals formed are relatively prone to experiencing the melting-recrystallization process. Furthermore, all the multiple melting peaks(T_m) of P(3,4)HB/PU composites move to higher temperature with the increase in PU content, which may be associated with the entanglement between the molecular chains of P(3,4)HB and PU. However, there are no endothermic melting peaks for PU in Figure 7(a), indicating that PU is amorphous, which is in accordance with XRD analysis.

The effect of PU on the crystallization behavior of P(3,4)HB was further studied by POM observation. Figure 8 shows the POM photographs of P(3,4)HB and P(3,4)HB/PU composites. The Maltese cross of P(3,4)HB spherulites could be clearly seen. In Figure 8(b–e) it is obvious that, with the incorporation of PU, the PU phase becomes noticeable in the polymer matrix, while the size of P(3,4)HB spherulites increases and the number of P(3,4)HB spherulites reduces significantly, which reveals that PU may retard P(3,4)HB crystallization. This is in agreement with the DSC results.

Thermal Stability of P(3,4)HB/PU Composites

The thermal stability of P(3,4)HB/PU composites were examined using TGA. Figure 9 shows TG and DTG curves for all samples and the results are summarised in Table IV. Obviously, a one-stage degradation process is observed for neat P(3,4)HB while a two-stage degradation process is observed for P(3,4)HB/PU composites. From Figure 9 and Table IV, it can be seen that the onset degradation temperature (T_{onset}, 5% mass loss) and the temperature at maximum mass loss rate (T_{max}) of P(3,4)HB/PU composites were increased with an increase in PU content. T_{onset} is increased from 227.7°C for neat P(3,4)HB to 230.0, 232.1, 235.4 and 236.7°C for P(3,4)HB-5, P(3,4)HB-10, P(3,4)HB-20 and P(3,4)HB-30, respectively. Both the hydrogen bond effect of the urethane group of PU with the hydroxyl of P(3,4)HB and the entanglement effect between two kinds of macromolecular chains may improve the thermal stability of the composites.

Biodegradability of P(3,4)HB/PU Composites

Microbial P(3,4)HB is one of the representative highly biodegradable plastics. The effect of polyester PU on the biodegradability of P(3,4)HB is of great interest. Firstly, we found that neat PU has a slow degradation rate and a small amount of weight loss (only 1.8 wt % after 10 days) in our activated sludge degradation test. The biodegradability of neat P(3,4)HB and P(3,4)HB/PU composites was also conducted. Figure 10 gives the weight loss curves of neat P(3,4)HB and P(3,4)HB/PU composites by activated sludge degradation. Apparently, the degradation rate of P(3,4)HB/PU composites is slower than that of neat P(3,4)HB and decreases with an increase in PU content. Neat P(3,4)HB degrades with a weight loss of 46.9 wt % after 10 days, while the composites have a weight loss of 44.3, 41.5, 36.9 and 27.8 wt % for P(3,4)HB-5, P(3,4)HB-10, P(3,4)HB-20 and P(3,4)HB-30, respectively.

Optical microscopy was used to observe the variation of surface morphology, with Figure 11 showing the surface morphology of P(3,4)HB and P(3,4)HB/PU composites before and after degradation. As shown in Figure 11(a_1–c_1), it can be seen that before activated sludge degradation, the surface morphology of the composites is smooth. However, after biodegradation, there is a significant change in the surface of the films, with holes appearing and a rougher-feature forming [Figure 11(a_2–c_2)].

CONCLUSIONS

A new type of PCL-based polyester polyurethane with 45 wt % hard segment component was successfully synthesized by a convenient method. P(3,4)HB/PU composites were prepared by solution casting and were well characterized. The results show that the amorphous PU elastomer can disperse well on the nanometer scale in the matrix, giving a microphase separated morphology. The crystal structure of P(3,4)HB does not change whereas its crystallization ability decreases. With the increase in PU content, the elongation at break of the composites is notably increased whereas the yield strength and elastic modulus are decreased. At the same time, the fracture characteristic of P(3,4)HB is obviously transformed from brittleness into ductility with the gradual increase of PU loading, which indicates that the PU elastomer has a notable toughening effect on P(3,4)HB. It can be concluded that when the synthesized PU is added, the P(3,4)HB/PU composites show obvious plastic deformation upon being subjected to tensile testing, which is an important energy-dissipation process and conducive to an increase in toughness of the matrix. Moreover, the thermal stability of P(3,4)HB/PU composites is improved obviously compared with that of pure P(3,4)HB. The activated sludge degradation test demonstrates that the biodegradability of P(3,4)HB/PU composites is decreased with an increase in PU content.

ACKNOWLEDGMENTS

This study was financially supported by and the Natural Science Foundation of Jiangsu Province (BK2012821) and the Project Funded by the Priority Academic Program Development (PAPD) of Jiangsu Higher Education Institutions.

REFERENCES

1. Demirbas, A. *Energ. Source. Part A* **2007**, *29*, 419.
2. Eyiler, E.; Chu, I. W.; Walters, K. B. *J. Appl. Polym. Sci.* **2014**, *131*, 40888.
3. Pederson, E. N.; McChalicher, C. W. J.; Srienc, F. *Biomacromolecules* **2006**, *7*, 1904.
4. Chanprateep, S.; Buasri, K.; Muangwong, A.; Utiswannakul, P. *Polym. Degrad. Stab.* **2010**, *95*, 2003.
5. Laycock, B.; Halley, P.; Pratt, S.; Werker, A.; Lant, P. *Prog. Polym. Sci.* **2013**, *38*, 536.
6. Philip, S.; Keshavarz, T.; Roy, I. *J. Chem. Technol. Biotechnol.* **2007**, *82*, 233.
7. Gao, X.; Chen, J. C.; Wu, Q.; Chen, G. Q. *Curr. Opin. Biotechnol.* **2011**, *22*, 768.
8. Luo, R. C.; Xu, K. T.; Chen, G. Q. *J. Appl. Polym. Sci.* **2007**, *105*, 3402.
9. Abe, H. *Macromol. Biosci.* **2006**, *6*, 469.
10. Cong, C. B.; Zhang, S. Y.; Xu, R. W.; Lu, W. C.; Yu, D. S. *J. Appl. Polym. Sci.* **2008**, *109*, 1962.
11. Sridhar, V.; Lee, I.; Chun, H. H.; Park, H. *Express. Polym. Lett.* **2013**, *7*, 320.
12. Ding, Y. C.; He, J. Y.; Yang, Y. Y.; Cui, S. J.; Xu, K. T. *Polym. Compos.* **2011**, *32*, 1134.
13. Wang, K. J.; Wang, Y. M.; Zhang, R.; Li, Q.; Shen, C. Y. *Polym. Compos.* **2012**, *33*, 838.
14. Zhang, R.; Huang, H.; Yang, W.; Xiao, X. F.; Yang, J.; Hu, Y. *High. Perform. Polym.* **2012**, *25*, 104.
15. Zhang, R.; Zhu, C. J.; Shan, X. Y.; Xia, J.; Zhu, Q.; Hu, Y. *J. Appl. Polym. Sci.* **2013**, *130*, 2015.
16. Li, Y. J.; Shimizu, H. *Macromol. Biosci.* **2007**, *7*, 921.
17. Gao, X. L.; Qu, C.; Fu, Q. *Polym. Int.* **2004**, *53*, 1666.
18. Han, J. J.; Huang, H. X. *J. Appl. Polym. Sci.* **2011**, *120*, 3217.
19. KrÓl, P. *Prog. Mater. Sci.* **2007**, *52*, 915.
20. Wang, S. H.; Silva, L. F.; Kloss, J.; Munaro, M.; Souza, G. P.; Wada, M. A.; Gomez, J. G. C.; Zawadzki, S.; Akcelrud, L. *Macromol. Symp.* **2003**, *197*, 255.

21. Khan, F.; Valere, S.; Fuhrmann, S.; Arrighi, V.; Bradley, M. *J. Mater. Chem. B* **2013**, *1*, 2590.

22. Báez, J. E.; Ramírez, D.; Valentín, J. L.; Ángle, M. F. *Macromolecules* **2012**, *45*, 6966.

23. Chan-Chan, L. H.; Correa, R. S.; Vargas-Coronado, R. F.; Cervantes-Uc, J. M.; Cauich-Rodríguez, J. V.; Quintana, P.; Bartolo-Pérez, P. *Acta Biomater.* **2010**, *6*, 2035.

24. Yu, L.; Li, W. W.; Lam, M. H. W.; Yu, H. Q. *Appl. Microbiol. Biotechnol.* **2011**, *90*, 1119.

25. Lu, X. P.; Wen, X.; Yang, D. *J. Mater. Sci.* **2011**, *46*, 1281.

26. Branciforti, M. C.; Corrêa, M. C. S.; Pollet, E.; Agnelli, J. A. M.; Nascente, P. A.; Avérous, L. *Polym. Test.* **2013**, *32*, 1253.

27. Wang, S. C.; Xiang, H. X.; Wang, R. L.; Peng, C.; Zhou, Z.; Zhu, M. F. *Polym. Eng. Sci.* **2014**, *54*, 1113.

28. Liu, T.; Petermann, J. *Polymer* **2001**, *42*, 6453.

29. Ding, C. K.; Cheng, B. W.; Wu, Q. *J. Therm. Anal. Calorim.* **2011**, *103*, 1001.